

## Damage detection in beam-like structures using deflections obtained by modal flexibility matrices

Ki-Young Koo\*

*Department of Civil & Environmental Engineering, KAIST, 373-1, Gusong-dong, Yusong-gu, Daejeon, Korea*

Jong-Jae Lee‡

*Civil & Environmental Engineering, Sejong University, 98 Gunja-dong, Kwangjin-gu, Seoul, Korea*

Chung-Bang Yun\*†

*Department of Civil & Environmental Engineering, KAIST, 373-1, Gusong-dong, Yusong-gu, Daejeon, Korea*

Jeong-Tae Kim\*\*

*Department of Ocean Engineering, Pukyong National University, 599-1 Daeyeon-dong, Namgu, Busan, Korea*  
(Received October 20, 2007, Accepted January 15, 2008)

**Abstract.** In bridge structures, damage may induce an additional deflection which may naturally contain essential information about the damage. However, inverse mapping from the damage-induced deflection to the actual damage location and severity is generally complex, particularly for statically indeterminate systems. In this paper, a new load concept, called the positive-bending-inspection-load (PBIL) is proposed to construct a simple inverse mapping from the damage-induced deflection to the actual damage location. A PBIL for an inspection region is defined as a load or a system of loads which guarantees the bending moment to be positive in the inspection region. From the theoretical investigations, it was proven that the damage-induced chord-wise deflection (DI-CD) has the maximum value with the abrupt change in its slope at the damage location under a PBIL. Hence, a novel damage localization method is proposed based on the DI-CD under a PBIL. The procedure may be summarized as: (1) identification of the modal flexibility matrices from acceleration measurements, (2) design for a PBIL for an inspection region of interest in a structure, (3) calculation of the chord-wise deflections for the PBIL using the modal flexibility matrices, and (4) damage localization by finding the location with the maximum DI-CD with the abrupt change in its slope within the inspection region. Procedures from (2)-(4) can be repeated for several inspection regions to cover the whole structure complementarily. Numerical verification studies were carried out on a simply supported beam and a three-span continuous beam model. Experimental verification study was also carried out on a two-span continuous beam structure with a steel box-girder. It was found that the proposed method can identify the damage existence and damage location for small damage cases with narrow cuts at the bottom flange.

**Keywords:** beam-like structures; deflection-based damage detection; modal flexibility; positive bending loads; outlier analysis; measurement noise; experiments.

---

\*Postdoctoral Researcher, E-mail: [kykoo@kaist.ac.kr](mailto:kykoo@kaist.ac.kr)

‡Professor, E-mail: [jongjae@sejong.ac.kr](mailto:jongjae@sejong.ac.kr)

\*†Professor, E-mail: [ycb@kaist.ac.kr](mailto:ycb@kaist.ac.kr)

\*\*Professor, E-mail: [idis@pknu.ac.kr](mailto:idis@pknu.ac.kr)

## 1. Introduction

Structural health monitoring (SHM) is an emerging subject in civil engineering, offering potential to prevent catastrophic structural failures, to increase cost effectiveness in maintenance, and to prolong the service life, by continuous and/or periodic assessments of the structural integrity of civil infrastructures. During the past three decades, vibration-based SHM methods have been extensively studied and developed utilizing various vibration characteristics such as natural frequencies, mode shapes, modal curvatures, modal flexibility, etc. An excellent review can be found in a report by Doebling *et al.* (1996). In spite of the in-depth research efforts in vibration-based SHM and damage detection methods, there still remain several challenges in the practical and reliable applications. Although many SHM methodologies have been devised, only a few have been fully validated for its applicability and reliability on site. Especially, from the viewpoint of online SHM frameworks, it is very important to detect damage or abnormality at the earliest stage to establish proper maintenance and/or retrofit plans on time. Therefore, it is highly required to adopt an appropriate damage detection method for the continuously or periodically incoming measurement data. More research efforts are also needed to enhance the applicability of the SHM technologies to real structure systems with a large number of degrees of freedom.

Recently, the modal flexibility has become one of the promising damage descriptors owing to its high sensitivity to damage. Through numerical studies for a spring-mass system with five degrees of freedom, Zhao and DeWolf (1999) showed that the modal flexibility is more sensitive for damage detection than the natural frequencies and mode shapes. Several damage detection methods have been proposed based on the modal flexibility. The earliest one is a damage detection method using changes in modal flexibility (Pandey and Biswas 1994). Anomaly in the uniform load surface calculated by modal flexibility was proposed as a damage feature (Toksoy and Aktan 1994). Damage detection method using changes in curvatures of the uniform load surface was also proposed (Zhang and Aktan 1995). The damage locating vector (DLV) was proposed to localize the damages based on changes in the modal flexibility with the intact finite element model (Bernal 2002). Many other methods have been also studied based on the modal flexibility (Madhwesh and Ahmet 1992, Yan and Golinval 2005, Ni, *et al.* 2008). The aforementioned methods have drawbacks such as the high noise sensitivity due to curvature calculations, the no explicit relationship between the damage and damage features, and the requirement of an intact finite element model.

The proposed method in this study is originated from the same idea with the method by Toksoy and Aktan (1994), but is based on the explicit relationship between the damage and damage-induced deflection. The load requirement for deflection-based damage detection is also theoretically investigated. In this paper, at first, the background theory is explained including the modal flexibility, the deflection estimation by the modal flexibility, the damage-induced deflection, and the deflection-based damage localization method. Then, numerical simulations are shown for a simply supported beam and a three-span continuous beam cases with noise-free measurement. Experimental verification study was also carried out on a two-span continuous beam structure with a steel box-girder. The proof for the proposed damage detection method is given in Appendix to make the main text simple and concise.

## 2. Theory

### 2.1. Deflection estimation by modal flexibility

The dynamic characteristic equation for a structure can be written as

$$\mathbf{M}\Psi\Lambda = \mathbf{K}\Psi \quad (1)$$

where  $\mathbf{M}$  and  $\mathbf{K}$  are the mass and stiffness matrices;  $\Psi$  is the un-scaled mode shape matrix which may be obtained by the output-only modal analysis (Peeters and De Roeck 2001, Brinker and Andersen 2002, Yi and Yun 2004); and  $\Lambda$  is the modal frequency matrix with  $\omega_i^2$  on its diagonal. When the un-scaled mode shape matrix  $\Psi$  is scaled to the mass-normalized mode shape matrix  $\Phi$  ( $\Phi^T\mathbf{M}\Phi = \mathbf{I}$ ), the stiffness matrix  $\mathbf{K}$  and the flexibility matrix  $\mathbf{G}$  can be expressed as

$$\mathbf{K} = \Phi^{-T}\Lambda\Phi^{-1} \quad (2)$$

$$\mathbf{G} = \Phi\Lambda^{-1}\Phi^T \quad (3)$$

The influence of the  $i$ -th mode on the stiffness matrix  $\mathbf{K}$  increases with the squares of the natural frequencies  $\omega_i^2$ , whereas the influence on the flexibility matrix  $\mathbf{G}$  decreases with  $\omega_i^{-2}$ . Therefore, the flexibility matrix can be constructed more accurately by using only a few lower modes than the stiffness matrix (Duan, *et al.* 2005, Gao, *et al.* 2006). The modal flexibility matrix  $\mathbf{G}_m$  using  $m$ -lower modes can be obtained as

$$\mathbf{G}_m = \Phi_m\Lambda_m^{-1}\Phi_m^T \quad (4)$$

where  $\Lambda_m = [\omega_i^2]$ ,  $\omega_i$  is the  $i$ -th natural frequency,  $i = 1, 2, \dots, m$ ;  $\Phi_m = [\phi_1, \phi_2, \dots, \phi_m]$ ; and  $\phi_i$  is the  $i$ -th mode shape with the mass-normalization which can be carried out by the added mass method (Brinker and Andersen 2002, Bernal 2004).

When the modal flexibility matrix is evaluated using Eq. (4), the deflection profile under an arbitrary load  $\mathbf{f}$  can be estimated by a simple matrix multiplication as

$$\mathbf{u} = \mathbf{G}_m\mathbf{f} \quad (5)$$

## 2.2. General equation of damage-induced deflection

For a structural system with a stiffness matrix  $\mathbf{K}_0$ , the relationship between the deflection  $\mathbf{u}_0$  due to a load  $\mathbf{F}$  can be expressed as

$$\mathbf{K}_0\mathbf{u}_0 = \mathbf{F} \quad (6)$$

A similar relationship can be obtained for a system with a structural damage defined as a reduction in the stiffness matrix  $\Delta\mathbf{K}$  as

$$(\mathbf{K}_0 - \Delta\mathbf{K})(\mathbf{u}_0 + \Delta\mathbf{u}) = \mathbf{F} \quad (7)$$

where  $\Delta\mathbf{u}$  is the damage-induced deflection caused by the damage  $\Delta\mathbf{K}$  under the same external force  $\mathbf{F}$ .

By subtracting Eq. (6) from Eq. (7) and applying the first order approximation, the general equation of the damage-induced deflection can be obtained as

$$\Delta\mathbf{u} = \mathbf{K}_0^{-1}(\Delta\mathbf{K}\mathbf{u}_0) = \mathbf{K}_0^{-1}\Delta\mathbf{F} \quad (8)$$

where  $\Delta \mathbf{F}$  is a part of the stress resultant which was caused by the damaged portion of the element under the undamaged condition. It may be also interpreted as the damage-equivalent force imposed on the damaged part of the structure. Eq. (8) indicates that the damage-induced deflection can be estimated by applying the damage-equivalent force on the undamaged structure.

For a special case with a damage at segment (e), the damage-equivalent force  $\Delta \mathbf{F}$  for a beam structure can be obtained as

$$\Delta \mathbf{F} = \Delta \mathbf{K} \mathbf{u}_0 = \begin{Bmatrix} 0 \\ \alpha_e \mathbf{f}^e \\ 0 \end{Bmatrix}$$

$$\Delta \mathbf{K} = \begin{bmatrix} 0 & 0 & 0 \\ 0 & \alpha_e \mathbf{k}^e & 0 \\ 0 & 0 & 0 \end{bmatrix} \quad (9)$$

where  $\mathbf{k}^e$  the intact stiffness matrix of the damaged segment (e);  $\alpha_e$  the damage index ( $0 < \alpha_e < 1$ ); and  $\mathbf{f}^e = \mathbf{k}^e \mathbf{u}_0^e = \{v_1, m_1, v_2, m_2\}^T$  is the stress resultant on the damaged element (e) for the external load  $\mathbf{F}$  under the undamaged state.  $v_1$  and  $m_1$  are the vertical forces and moments at the left end of (e) and  $v_2$  and  $m_2$  are those at the right end of (e); and  $\mathbf{u}_0^e$  is the nodal deflection of the element (e) under the undamaged state. From Eq. (9), it is noticed that the damage-equivalent force  $\Delta \mathbf{F}$  acts only on the damaged segment not on the rest of the structure.

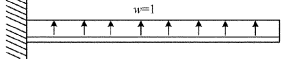
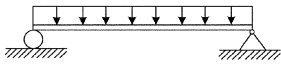
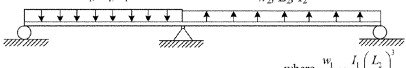
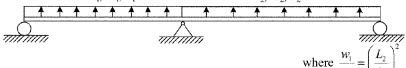
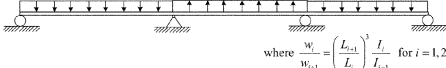
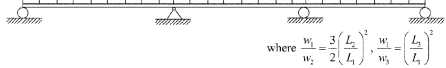
### 2.3. Positive bending inspection load

The inflection point is the point where the curvature of the deflection and the bending moment are zero. It is worthy to note that damage near an inflection point may not induce significant additional deflection to the beam structure because the bending moment on the damaged portion is negligibly small. Therefore, it is almost impossible to detect damages near the inflection points using the damage-induced deflection. To detect the damage in a region of interests, a load or a system of loads producing no inflection point in the region is desirable. For this end, a positive-bending-inspection-load (PBIL) is proposed in this study, which guarantees the positive bending moment in the inspection region, so that no inflection point may occur in that region.

Examples of the loads satisfying the requirement of the bending moment positiveness are shown in Table 1. Span-wise uniform loads are considered in this study for the simplicity of definition and manipulation. For a cantilever and a simply supported beam, a uniform load on the whole beam length does not produce any inflection point. For a continuous beam system, however, there is no single uniform load for the entire beam length, which prevents inflection points over the whole structure. Therefore, two types of loads, namely span inspection load  $f^1$  and intermediate support inspection load  $f^2$ , are devised as shown in Table 1.

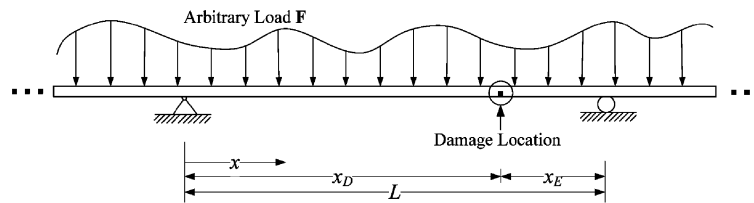
The span inspection load  $f^1$  as shown in Table 1 produces inflection points only at the intermediate supports, while the intermediate support inspection load  $f^2$  produces the maximum positive moment at the intermediate supports. The magnitudes of the span-wise uniform loads  $w_i$ ,  $i = 1, 2$  can be determined using the formula shown in Table 1 for the cases with a span-wise uniform cross-section. Two loads  $f^1$  and  $f^2$  may be utilized complementarily to detect damage at an arbitrary location within the whole

Table 1 Examples of PBILs for various inspection regions

Beam Types	Inspection Regions $\Omega$	PBILs	Definitions of inspection loads
Cantilever Beam	Whole structure	$f^{1,*}$	$(f^1)$ 
Simply Supported Beam	Whole structure	$f^1$	$(f^1)$ 
2-Span Continuous Beam	1 <sup>st</sup> span-region	$f^1$	$(f^1)$ 
	2 <sup>nd</sup> span-region	$-f^1$	
	Intermediate support-region <sup>**</sup>	$f^{2,*}$	$(f^2)$ 
3-Span Continuous Beam	1 <sup>st</sup> and 3 <sup>rd</sup> span-regions	$f^1$	$(f^1)$ 
	2 <sup>nd</sup> span-region	$-f^1$	
	Intermediate support-regions <sup>**</sup>	$f^2$	$(f^2)$ 

<sup>\*)</sup>  $f^1$  and  $f^2$ : Span-region inspection load and intermediate support-region inspection load.

<sup>\*\*</sup>) Intermediate support-region may cover the 1/4 span regions on both sides of the support


 Fig. 1 Continuous beam system with damage under an arbitrary load  $F$ 

beam. For cases with non-uniform cross-sections in a span, proper PBILs can be easily devised by structural analysis, which should satisfy the requirement of the moment positiveness within their own regions of interest.

#### 2.4. Equation of damage-induced deflection for continuous beams

Consider a continuous beam with a single damage loaded by an arbitrary load  $F$  as shown in Fig. 1. The damage is assumed to locate at  $x = x_D$  having very small damage-width.

A span with the damage can be regarded as an equivalent single-span beam with two rotational springs  $k_A$  and  $k_B$  at the supports as shown in Fig. 2(a). As discussed in the previous section, the

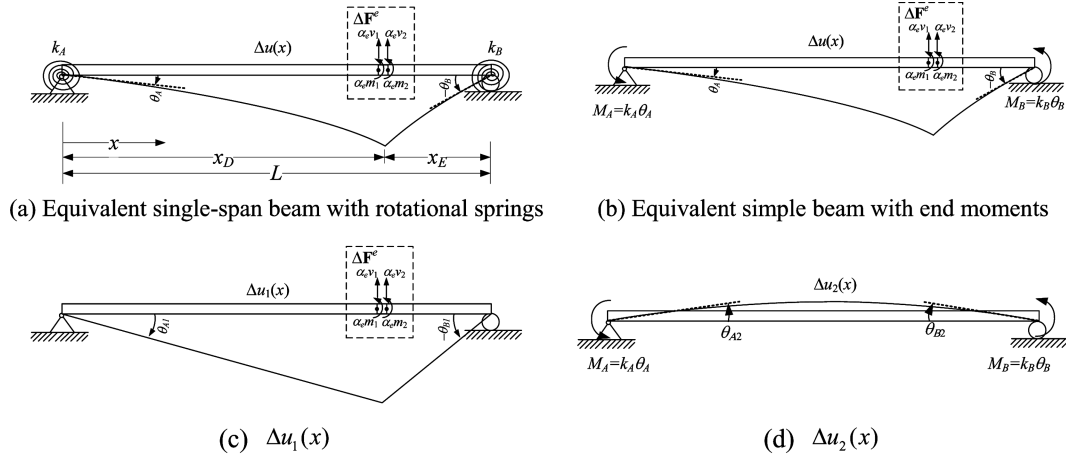


Fig. 2 Equivalent simple beam for calculation of damage-induced deflections

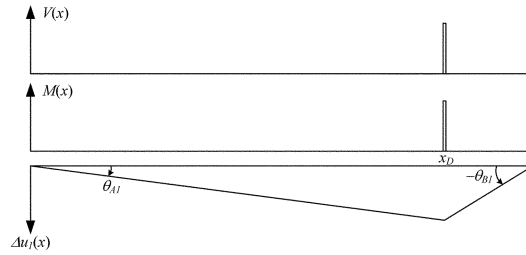


Fig. 3 Shear stresses, bending moments, and the damage-induced deflection

damage-induced deflection can be obtained by applying the damage-equivalent load  $\Delta \mathbf{F}^e = \alpha_e \{v_1, m_1, v_2, m_2\}^T$  to the single-span beam in the intact condition as shown in Fig. 2(a), where the signs of the internal forces are defined as in the conventional finite element analysis.

For the convenience of analysis, further simplification has been made by replacing the rotational springs  $k_A$  and  $k_B$  with two end reaction moments  $M_A = k_A \theta_A$  and  $M_B = k_B \theta_B$ , which occur in the simple beam as shown in Fig. 2(b). Then, the damage-induced deflection shown in Fig. 2(b) can be obtained by summing two deflections; i.e.,  $\Delta u_1(x)$  of the simple beam under  $\Delta \mathbf{F}^e$  as in Fig. 2(c), and  $\Delta u_2(x)$  under  $M_A$  and  $M_B$  as in Fig. 2(d), so long as the resulting rotations at the ends  $\theta_A$  and  $\theta_B$  are same as those in Fig. 2(a).

#### 2.4.1. Calculation of $\Delta u_1(x)$

The damage equivalent force  $\Delta \mathbf{F}^e$  is a self-equilibrium force. Thus, when  $\Delta \mathbf{F}^e$  is applied to the simple beam shown in Fig. 2(c), no reaction forces are produced at the supports, and no shear force and bending moment are produced along the beam except at the damage location  $x = x_D$  as shown in Fig. 3.

The deflection  $\Delta u_1(x)$  by  $\Delta \mathbf{F}^e$  is a triangular shape except at the damage location, which can be expressed by two linear curves as

$$\Delta u_1(x) = \begin{cases} \theta_{A1} x & 0 \leq x < x_D \\ -\frac{x_D}{x_E} \theta_{A1} (x - L) & x_D \leq x < L \end{cases} \quad (10)$$

where  $\theta_{A1}$  and  $\theta_{B1}$  are the end rotations with  $\theta_{B1} = -(x_D/x_E)\theta_{A1}$  as in Fig. 3.

In Eq. (10),  $\Delta u_1(x)$  is expressed in terms of  $\theta_{A1}$ . Hereafter, the deflection equations will be expressed in terms of  $\theta_{A1}$  for the simplicity and convenience. The sign of  $\theta_{A1}$  is dependent on the sign of the bending moment of  $\Delta F^e$ . In other words, if the bending moment is positive,  $\theta_{A1}$  is positive, while if the bending moment is negative,  $\theta_{A1}$  is negative.

#### 2.4.2. Calculation of $\Delta u_2(x)$

To calculate  $\Delta u_2(x)$  of the idealized simple beam, the end rotations  $\theta_A$  and  $\theta_B$  are needed to determine the applied moments at the ends,  $M_A = k_A \theta_A$  and  $M_B = k_B \theta_B$ , as shown in Fig. 2(d). The end rotations can be obtained by solving the following equations: Eq. (11a) describing that the end rotations in  $\Delta u(x)$  is the sum of those in  $\Delta u_1(x)$  and  $\Delta u_2(x)$ ; Eq. (11b) for the end rotations of the beam due to  $M_1$  and  $M_2$ ; and Eq. (11c) for the stiffness of the rotational springs as

$$\theta = \theta_1 - \theta_2 \quad (11a)$$

$$\theta_2 = \mathbf{g} \mathbf{m} \quad (11b)$$

$$\mathbf{m} = \mathbf{k} \theta \quad (11c)$$

where  $\theta = \{\theta_A, \theta_B\}^T$ ,  $\theta_1 = \{\theta_{A1}, \theta_{B1}\}^T$ , and  $\theta_2 = \{\theta_{A2}, \theta_{B2}\}^T$  are the end rotations in  $\Delta u(x)$ ,  $\Delta u_1(x)$ , and  $\Delta u_2(x)$ ;  $\mathbf{m} = \{M_A, M_B\}^T$  is the end moments;  $\mathbf{k} = \text{diag}(k_A, k_B)$ , and  $\mathbf{g}$  is the rotational flexibility matrix with respect to the end moments as

$$\mathbf{g} = L/3EI \times \begin{bmatrix} 1 & -1/2 \\ -1/2 & 1 \end{bmatrix} \quad (11d)$$

in which  $EI$  is the bending rigidity of the beam section.

By solving the above equations, the moment vector  $\mathbf{m}$  can be obtained in terms of  $\theta_1$  as

$$\mathbf{m} = \mathbf{k} \theta = \mathbf{k}(\mathbf{I} + \mathbf{g} \mathbf{k})^{-1} \theta_1 \quad (12)$$

where  $\mathbf{I}$  is the 2 by 2 identity matrix.

When the cross sections of the beam is assumed to be uniform, the deflection  $\Delta u_2(x)$  due to  $M_A$  and  $M_B$  can be obtained as

$$\Delta u_2(x) = -\frac{Lx}{3EI} \left( 1 - \frac{3}{2}(x/L) + \frac{1}{2}(x/L)^2 \right) M_A + \frac{Lx}{6EI} (1 - (x/L)^2) M_B \quad (13)$$

which can be rewritten in terms of  $\theta_{A1}$  using Eq. (12) as

$$\Delta u_2(x) = \frac{\theta_{A1}}{3EI(4 + 4k_A + 4k_B + 3k_A k_B)x_E L} xP(x) \quad (14)$$

where

$$P(x) = ax^2 + bx + c$$

$$\begin{aligned}
a &= -2x_E x_A + 2x_D k_B + 3(x_D - x_E) k_A k_B \\
b &= 6x_E L k_A - 3(x_D - 2x_E) L k_A k_B \\
c &= -4x_E L^2 k_A - 3x_D L^2 k_B + 3x_E L^2 k_A k_B
\end{aligned} \tag{15}$$

Finally, the damage-induced deflection is obtained by the sum of the two deflections as

$$\Delta u(x) = \Delta u_1(x) + \Delta u_2(x) \tag{16}$$

### 2.5. Damage localization by damage-induced deflection

To make the damage localization procedure effectively, a damage-induced chord-wise deflection (DI-CD)  $\Delta u_\Omega(x)$  is introduced, which can be defined as the additional deflection measured from the chord connecting two points at  $x = x_a$  and  $x_b$  as

$$\Delta u_\Omega(x) = \Delta u(x) - \left( \frac{\Delta u(x_b) - \Delta u(x_a)}{x_b - x_a} (x - x_a) + \Delta u(x_a) \right) \tag{17}$$

where  $\Omega = [x_a, x_b]$  is the inspection region.

From the theoretical investigation on the DI-CD, the damage localization algorithm can be established using  $\Delta u_\Omega(x)$  as follows.

$$\text{Damage occurs at } x = x_D \Leftrightarrow \begin{cases} \Delta u_\Omega(x) \text{ has the maximum at } x = x_D \text{ and} \\ \Delta u'_\Omega(x) \text{ changes abruptly at } x = x_D \text{ under a PBIL} \end{cases} \tag{18}$$

where a PBIL is a positive-bending-inspection-load in the inspection region  $\Omega$  which guarantees the moment positiveness in  $\Omega$ , as defined in the previous section and illustrated in Table 1. Eq. (18) states

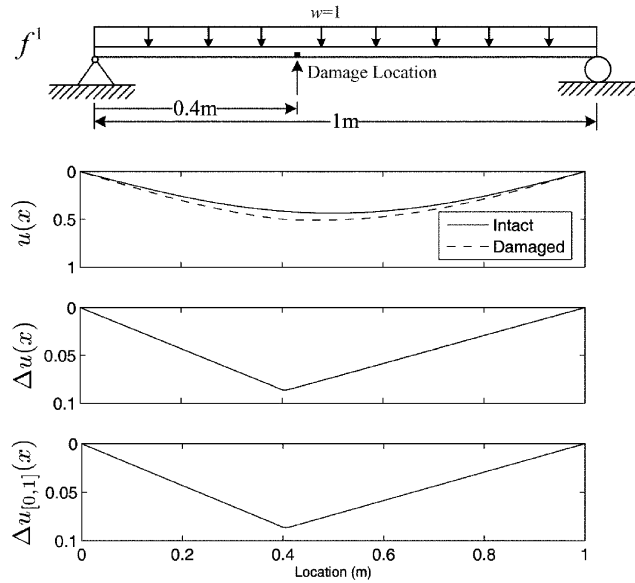


Fig. 4 Example of damage-induced chord-wise deflection for a simply support beam



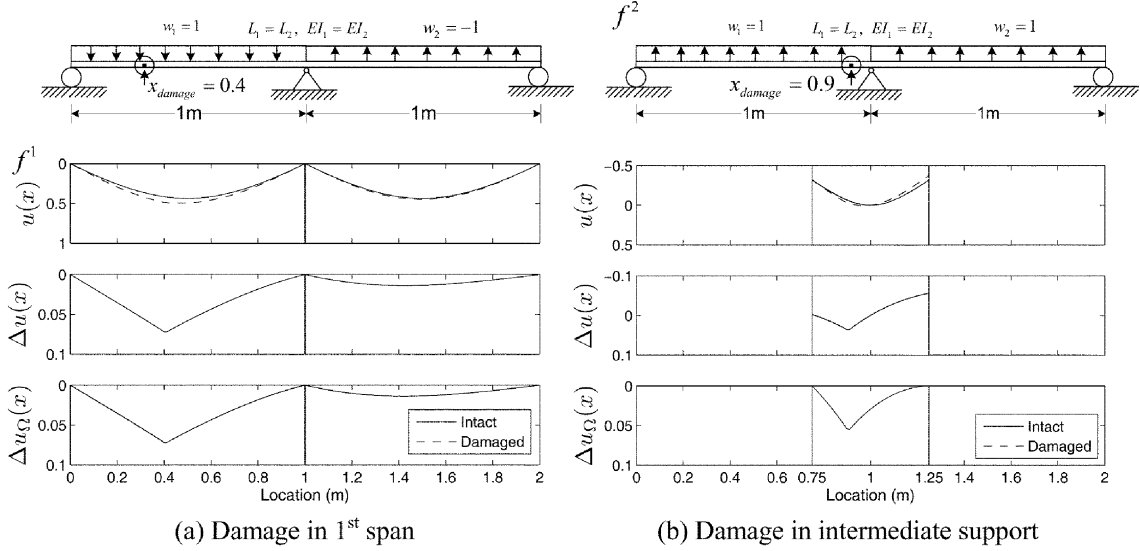


Fig. 5 Examples of damage-induced chord-wise deflections for a 2-span continuous beam

that the damage can be localized at the location with the maximum DI-CD  $\Delta u_{\Omega}(x)$  and the abrupt change in its slope. The proof of Eq. (18) is described in Appendix, and two illustrative examples are shown in Figs. 4-5. For a damage near a mid-span, the inspection region is taken as the whole span of interest. On the other hand, for a damage near an intermediate support region, the inspection region is taken as the 1/4 span regions on both sides of the support.

## 2.6. A proposed method under measurement noises

In realization of Eq. (18) for damage detection, statistical approaches are preferred due to inevitable measurement noises. A novelty index  $Z_i$  of the damage-induced chord-wise deflections is utilized to alarm the damage existence as follows

$$\text{Damage existence alarm issues if mean } (Z_i) > Z^{\text{Threshold}} \quad (19)$$

$$Z_i = \frac{u_{\Omega}(x_i) - \bar{u}_{\Omega}^I(x_i)}{\sigma(u_{\Omega}^I(x_i))}, x_i \in \Omega \quad (20)$$

$$u_{\Omega}(x_i) = u(x) - \left( \frac{u(x_b) - u(x_a)}{x_b - x_a} (x - x_a) + u(x_a) \right) \quad (21)$$

$$u = G_m f_{PBIL} \quad (22)$$

where  $\Omega = [x_a, x_b]$  is the inspection region;  $Z_i$  is the novelty index of the damage-induced chord-wise deflection  $u_{\Omega}(x)$  at the location  $x_i \in \Omega$ ;  $u_{\Omega}(x_i)$  is the concurrent chord-wise deflection in  $\Omega$ ,  $x_i \in \Omega$ ;  $\bar{u}_{\Omega}^I(x_i)$  is the mean-value of the referenced (intact) chord-wise deflection  $u_{\Omega}^I(x_i)$  over measurements;  $\sigma(u_{\Omega}^I(x_i))$  is the standard deviation of  $u_{\Omega}^I(x_i)$ ;  $u(x)$  is the deflection under  $f_{PBIL}$ ;  $f_{PBIL}$  is the PBIL for the inspection region  $\Omega$ ; and  $G_m$  is the modal flexibility.

When a damage existence has been found in the inspection region  $\Omega$ , the damage localization shall be

followed. Herein, to account for the inevitable measurement noise again, the damage-induced chord-wise deflection is evaluated using Eq. (23) based on the mean values of the damage-induced chord-wise deflections as

$$\Delta \bar{u}_{\Omega}(x_i) = \bar{u}_{\Omega}^D(x_i) - \bar{u}_{\Omega}^I(x_i) \quad (23)$$

where  $\Delta \bar{u}_{\Omega}(x_i)$  is the mean-change in the damage-induced chord-wise deflection;  $\bar{u}_{\Omega}^D(x_i)$  is the mean-value of  $u_{\Omega}(x_i)$  after issuing damage existence alarm; and  $\bar{u}_{\Omega}^I(x_i)$  is the mean-value for the reference case.

According to Eq. (23), the location of the maximum DI-CD,  $x_m = \arg \max_{x_i} \Delta \bar{u}_{\Omega}(x_i)$  is assessed to be an actual damage location, if the abrupt change in the slope of  $\Delta u_{\Omega}(x)$  occurs at  $x_m$ . However, if  $\Delta u_{\Omega}(x)$  does not come with an abrupt change at  $x_m$ , it can be assessed the damage might have occurred outside the inspection region  $\Omega$ .

The proposed damage localization can be summarized as follows.

$$\begin{aligned} \text{Damage locates at } x_m & \quad \text{if } I_A(x_m) \geq I_A^{Threshold} \\ \text{Damage locates outside of } \Omega & \quad \text{if } I_A(x_m) < I_A^{Threshold} \end{aligned} \quad (24)$$

where  $I_A(x_m)$  is an index to measure the abrupt change in the slope of  $\Delta \bar{u}_{\Omega}(x)$  at  $x = x_m$ . An index is proposed based on the area ratio without explicit calculations of the slope as follows.

$$I_A(x_m) = 1 - \frac{\int_{\Omega} \Delta \bar{u}_{\Omega}(x) dx}{\int_{\Omega} \Delta \bar{u}_{\Omega}(x_m) dx} \quad (25)$$

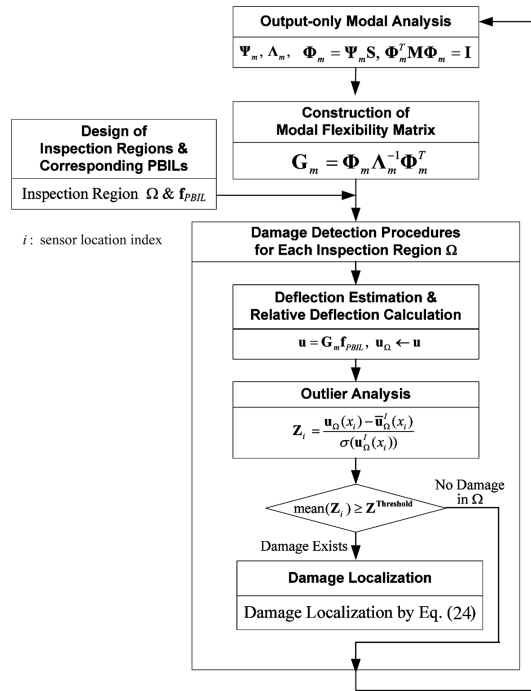


Fig. 6 The flow chart of the proposed method

For the case of the abrupt change in the slope in  $\Omega$ ,  $\Delta u_{\Omega}(x_i)$  will be a triangular shape or peaked-shape resulting into  $I_A \geq 0.5$ . On the other hand, for the case of no abrupt change in the slope in  $\Omega$ ,  $\Delta u_{\Omega}(x_i)$  will have a smooth convex curve resulting into  $I_A < 0.5$ . Typical example for each case can be seen in  $\Omega_{[0,1]}$  and  $\Omega_{[1,2]}$  of Fig. 5(a), respectively. The proposed damage detection procedure is summarized in Fig. 6.

### 3. Numerical study

#### 3.1. Simply supported beam structure

Numerical investigation on the proposed damage localization algorithm by Eq. (18) was carried out on a simply supported beam with a uniform cross section ( $EI=\text{constant}$ ) under the PBIL  $f^1$  as shown in

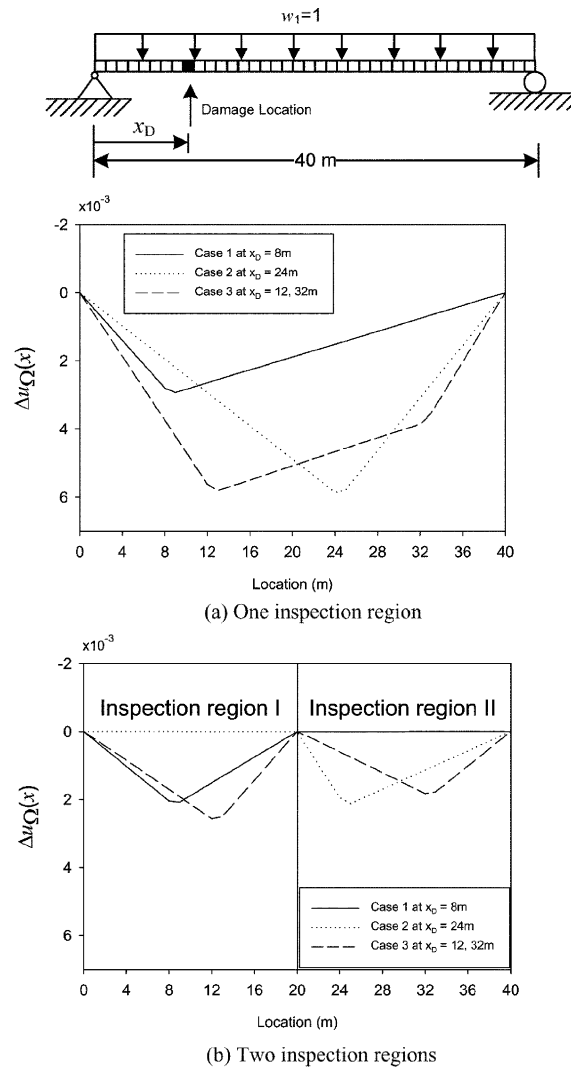


Fig. 7 DI-CWDs for a simply supported beam

Table 1. The structure is modeled by 40 beam elements. Two single damage cases with 10%  $EI$  reduction and one double damage case with 10%  $EI$  reduction each at different locations were considered as shown in Fig. 7. Two single damages locate at  $x_D = 8$  and 24 (m) respectively and one double damage locates at  $x_D = 12$  and 32 (m) simultaneously. Acceleration measurements were assumed available at 41 node locations without noise for sufficiently long duration. The first three natural frequencies and mode shapes were utilized to construct the modal flexibility matrices before and after damage, and then the deflections are estimated by using the modal flexibility matrices and a uniform load which is a PBIL for this case. The deflections are scaled with a constant so that the maximum value is to be 1. The DI-CDs defined in the whole structure and the two inspection regions are shown in Figs. 7(a) and 7(b), respectively. For the single damage cases, it can be found that the damage can be localized at the location where the DI-CD is the maximum and its slope changes abruptly as shown in both inspection regions. For the double damage case, it can be found that the damage can be localized by using two separated inspection regions as shown in Fig. 7(b).

### 3.2. Continuous beam structure with 3 spans

A three-span continuous beam model with a uniform cross section ( $EI = \text{constant}$ ) is considered. The structure is modeled by 122 beam elements. Nine damage cases of 20%  $EI$  reduction at different locations were considered as shown in Fig. 8:  $x_D = 10, 19, 29, 33, 38, 42, 50, 61$  and 72 m. The first four natural frequencies and mode shapes were assumed to be evaluated exactly, and they were utilized to construct the modal flexibility matrices before and after damage for each case. The deflections under PBILs are estimated by the modal flexibility matrices and are scaled so that the maximum deflection value is to be 1. The damage-induced chord-wise deflections are shown for the 5 inspection regions ( $\Omega_1 - \Omega_5$ ) in Fig. 9.

Fig. 9(a) shows the damage-induced chord-wise deflections  $\Delta u_{\Omega_i}(x)$  in five inspection regions due to damage in the 1st span. By inspecting  $\Delta u_{\Omega_1}(x)$  of the 1st span, the damages occurred in the 1st span were able to be clearly identified and localized by the locations of the maximum deflections with the abrupt changes in the slope. However,  $\Delta u_{\Omega_i}(x)$  in the other regions  $\Omega_i$  ( $i = 2, 3, 4, 5$ ) are found to be smooth without the abrupt changes in the slopes, which indicates no existence of damage in those spans.

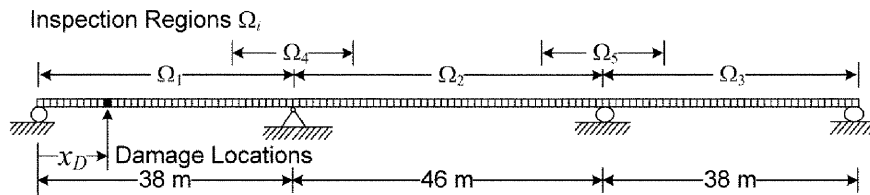


Fig. 8 A three span continuous beam model with different damage cases

Table 2 Inspection regions and corresponding PBILs for a 3-span continuous beam model

Inspection Regions $\Omega_i$ *)	PBILs
$\Omega_1$ and $\Omega_3$	$f^1$
$\Omega_2$	$f^1$
$\Omega_4$ and $\Omega_5$	$f^2$

\*)Definitions of  $\Omega_i$  are shown in Fig. 5, and  $f^i$  are defined in Table 1.

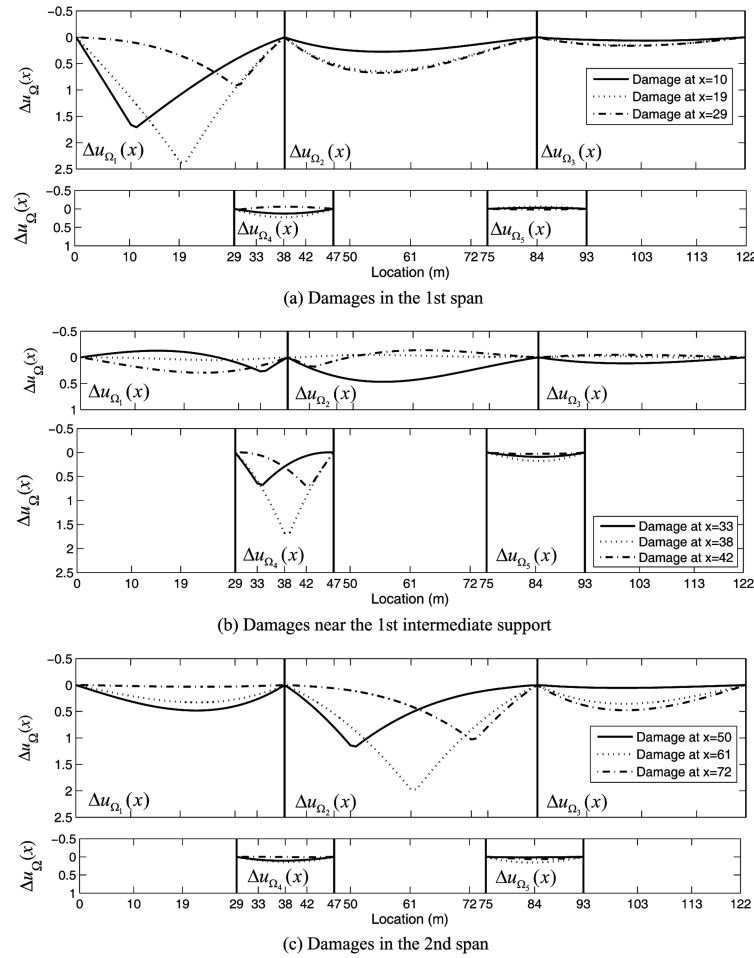


Fig. 9 Damage-induced chord-wise deflections for a three-span continuous beam system

Fig. 9(b) shows  $\Delta u_{\Omega_1}(x)$  due to damages around the 1st intermediate support. It can be found that the damages near the support were clearly identified and localized by checking  $\Delta u_{\Omega_1}(x)$ . It is worthy to note that  $\Delta u_{\Omega_1}(x)$  and  $\Delta u_{\Omega_2}(x)$  for the 1st and 2nd span regions can also indicate the damage occurrences at  $x = 33$  and  $42$  m. But the peaks are relatively small, since the damages occurred near the inflection point at the 1st intermediate support under the span PBILs.

Fig. 9(c) shows similar results for the damages occurred in the center span, which also demonstrate the effectiveness of the present damage-induced chord-wise deflection method incorporating PBILs.

#### 4. Experimental study

Experimental validation of the proposed method was carried out on a steel box-girder model shown in Fig. 10. The test structure is a two-span continuous box-girder model of 18 m long, which is composed of 9 segmental boxes connected by bolts and plates. Detailed dimensions of the test structure were given at Fig. 10(a). Nineteen accelerometers were evenly placed on the upper surface of one side

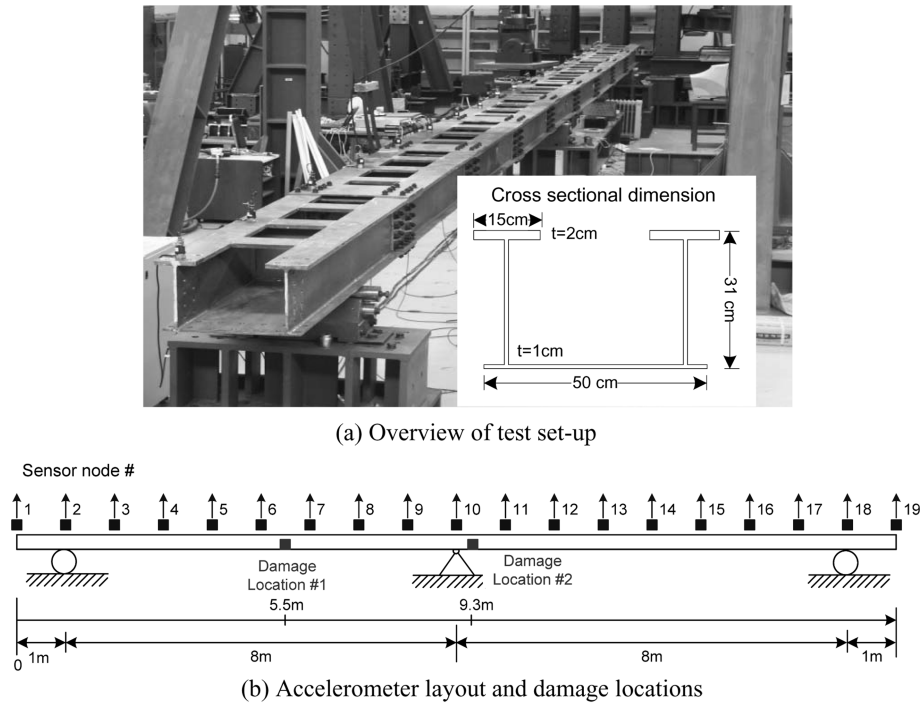


Fig. 10 Laboratory test on a steel-box girder model

Table 3 Damage severity on test section

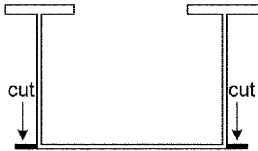
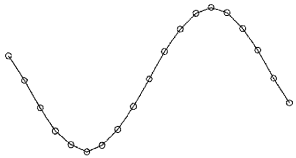
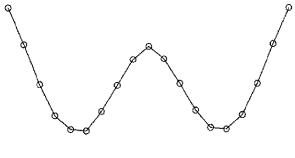
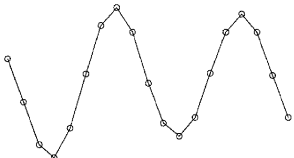
Item	Description
Section Shape	
Description	a cut of 5.0 cm long and 1 mm wide on each side
Bending Rigidity ( $EI$ )	12% Reduction in the cut-section
Area	4.6% Reduction

Table 4 Damage scenarios

Damage cases	Damage scenario
Damage 1	at Location 1
Damage 2	at Location 1 and 2

of the box-girder as shown in Figs. 10(a) and 10(b). Small damages of narrow cuts were imposed at two locations on the bottom flange by saw cuts as described in Tables 3 and 4. Vibration responses were induced by successive impact loads during 4 minutes, and the acceleration responses were measured with 200 Hz sampling rate. An example record is shown in Fig. 11. The acceleration measurements were repeated 18 times for the intact case and 7 times for each damage case. The experiments were

Table 5 Modal parameters extracted by EFDD before and after damages

	Mode 1			Mode 2			Mode 3		
	13.599 (Hz)			20.263 (Hz)			51.689 (Hz)		
Intact									
Damage Cases	Frequency $f_i$ (Hz)	$\Delta f_i/f_i^*$ (%)	MAC**	Frequency $f_j$ (Hz)	$\Delta f_j/f_j$ (%)	MAC	Frequency $f_3$ (Hz)	$\Delta f_3/f_3$ (%)	MAC
Damage 1	13.592	-0.05	1.0000	20.258	-0.02	1.0000	51.666	-0.01	0.9999
Damage 2	13.594	-0.04	1.0000	20.250	-0.06	1.0000	51.691	0.00	0.9999

<sup>\*</sup>)  $\Delta f_i$  from the intact values  $f_i$ .

<sup>\*\*</sup>) MAC between the modes before and after damage.

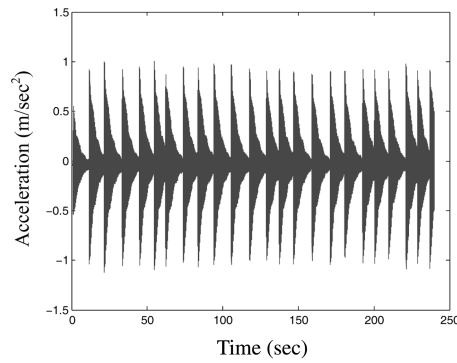


Fig. 11 Typical example acceleration time history

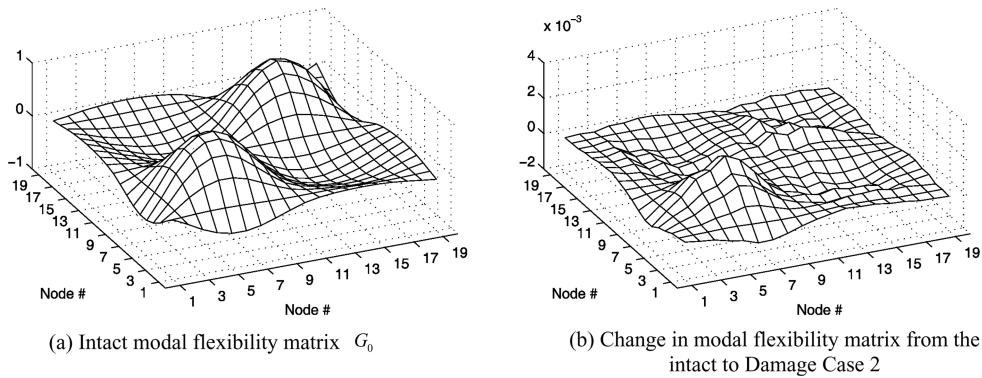


Fig. 12 Modal flexibility matrix and its change due to Damage Case 2

performed during a period of about 6 hours, while the temperature remains nearly steady to make temperature effects negligible.

Modal parameters were extracted using the enhanced frequency domain decomposition (EFDD)

Table 6 PBILs for test bridge

Inspection Regions	PBILs	Definition of PBIL
1 <sup>st</sup> span-region	$f^1$	
2 <sup>nd</sup> span-region	$-f^1$	
Intermediate support-region	$f^2$	

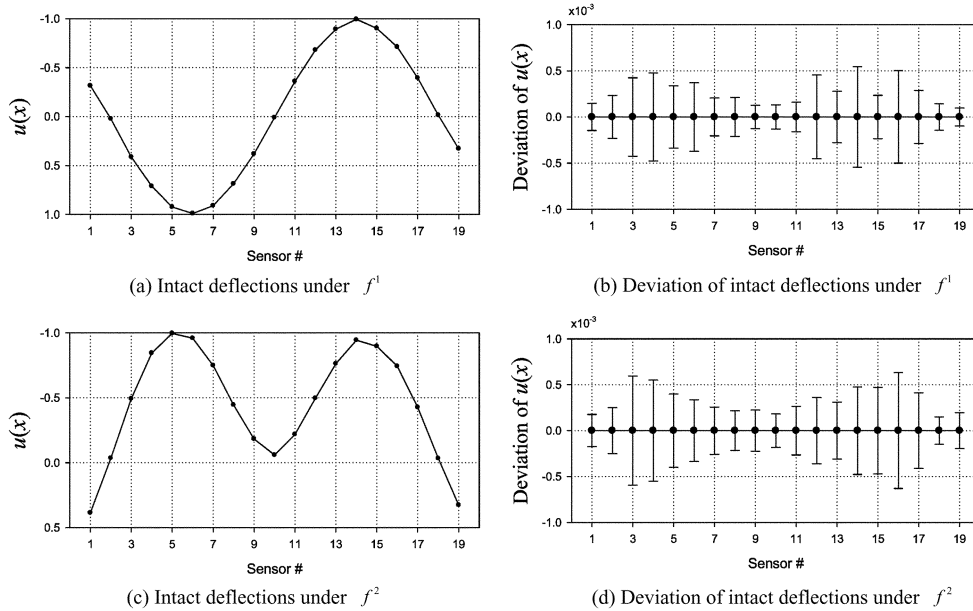


Fig. 13 Eighteen sets of the intact deflections and their deviation level under PBILs

method (Brincker, *et al.* 2001), which can estimate natural frequencies accurately using curve fitting in time domain. Typical modal parameters estimated are shown in Table 5. The modal assurance criterion (MAC) values were obtained between the mode shapes of the intact and damage cases. The changes in natural frequencies and mode shapes due to the damage were found to be very small. Accordingly it will be very difficult to detect the damage directly based on the modal parameters.

The modal flexibility matrices were constructed by using Eq. (4) for the intact and damaged cases based on the mass-normalized mode shapes. The mass normalization was carried out by using the lumped mass matrix obtained from the design drawing of the test structure. The typical modal flexibility matrix for the intact case and the typical change in the modal flexibility matrices are shown in Fig. 12. The modal flexibility matrix was scaled to have a unit-maximum value.

The PBILs  $f_{PBIL}$  used for the test structure are shown in Table 6. The deflections under the PBILs  $f_1$  and  $f_2$  were calculated for 18 sets of the modal flexibility matrices obtained from the intact



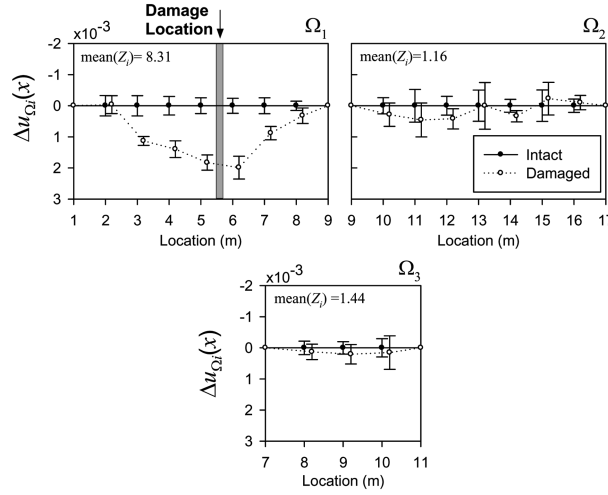
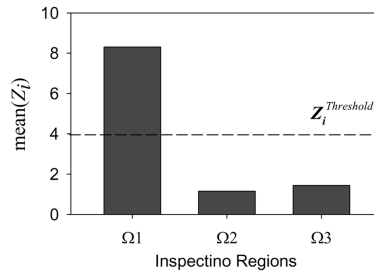

 Fig. 14 Means and  $2\sigma$  deviations in the DI-CDs for Damage Case 1 from Intact Case


Fig. 15 Damage existence assessment for Damage Cases 1 from Intact Case

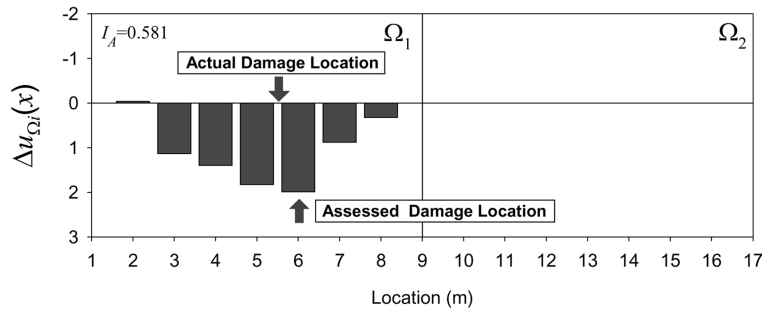


Fig. 16 Damage localization assessment for Damage Cases 1 from Intact Case

measurements as shown in Fig. 13. The results were scaled so that the absolute maximum value are to be 1.0. As seen in the Fig. 13, eighteen results almost coincide with each other and the deviation levels are less than  $\pm 0.8 \times 10^{-3}$ , which indicates the excellent repeatability of the estimated deflections.

For Damage Cases 1 and 2, the chord-wise deflection changes in each inspection region are shown in Figs. 14, 17 and 20. For Damage Case 1 with a small narrow cut at  $x_D = 5.5$  in the 1st span, the chord-wise deflection in the 1st span increased very significantly with an abrupt change in the slope near the damage location, while small change occurred in the other two regions without damages as shown in

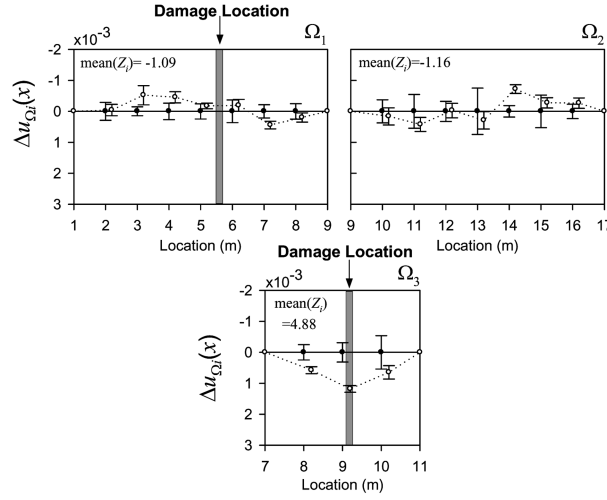
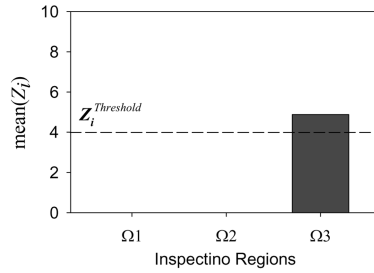
Fig. 17 Means and  $2\sigma$  deviations in the DI-CDs for Damage Case 2 from Damage Case 1

Fig. 18 Damage existence assessment for Damage Cases 2 from Damage Case 1

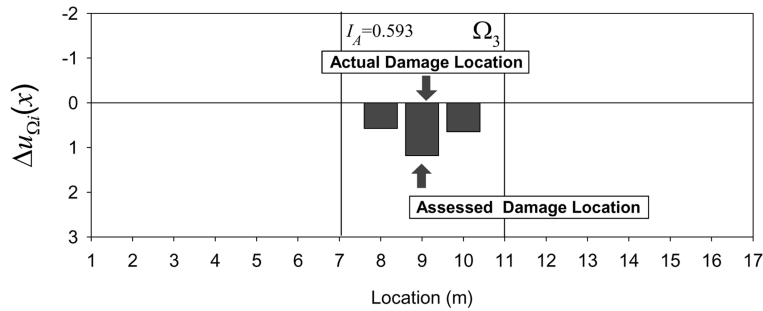


Fig. 19 Damage localization assessment for Damage Case 2 from Damage Case 1

Fig. 14. The novelty indices were calculated by using Eq. (20) and its mean values were shown in Fig. 15. Damage existence alarm issued in  $\Omega_1$  with  $Z_i^{Threshold} = 4$ . The index of the abrupt change was  $I_A(x_m = 6) = 0.581 > 0.5$ , so the damage location was assessed to be  $x_m = 6(m)$  which is reasonable since it is one of the closest measured-location to the actual damage location at  $x_D = 5.5(m)$ .

For Damage Case 2 with an additional small cut near the intermediate support, very visible increase can be observed in the chord-wise deflection under the PBIL in the intermediate support region, while no significant increases in the other regions without damages. The mean values of the novelty indices

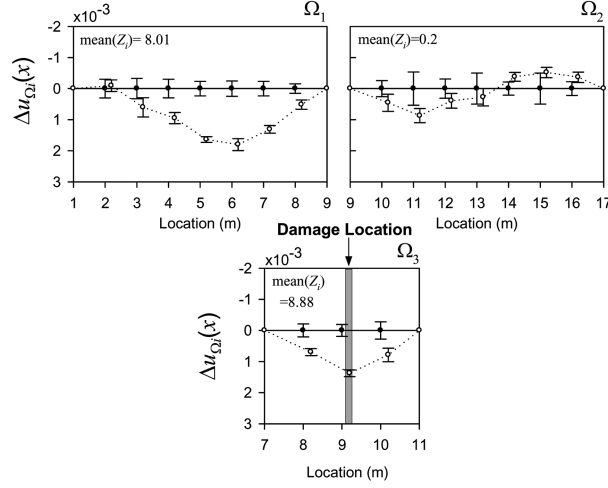
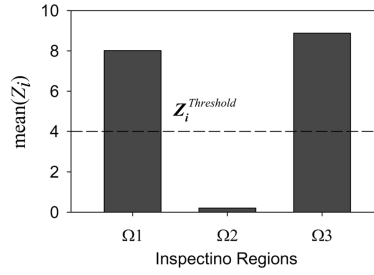

 Fig. 20 Means and  $2\sigma$  deviations in the DI-CDs for Damage Case 2 from Intact Case


Fig. 21 Damage existence assessment for Damage Cases 1 from Intact Case

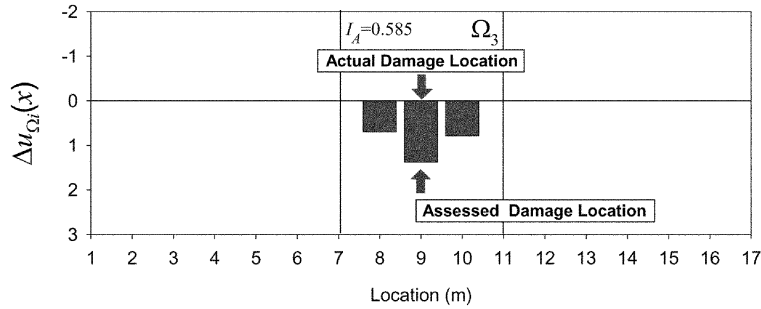


Fig. 22 Damage localization assessment for Damage Case 2 from Intact Case

were shown in Fig. 18. Damage existence alarm issued in  $\Omega_3$ , and the index of the abrupt change was  $I_A(x_m = 9) = 0.593 > 0.5$ . Thus the damage location was assessed to be  $x_m = 9(\text{m})$ , which is reasonable since it is the closest measured-location to the actual damage location at  $x_D = 9.3(\text{m})$ .

Fig. 20 shows the chord-wise deflection increase of Damage Case 2 from Intact Case under the PBIL. Two visible increases were observed on both the 1<sup>st</sup> span and the intermediate support region, while no significant increases in the 2<sup>nd</sup> span region without damage. The mean values of the novelty indices were shown in Fig. 21. Damage existence alarm issued in both  $\Omega_1$  and  $\Omega_3$ , and the indices of the abrupt

change were  $I_A(x_m = 6) = 0.586 > 0.5$ , and  $I_A(x_m = 9) = 0.585 > 0.5$ . Thus the damage locations were assessed to be  $x_m = 6$  and  $9$  (m).

## 5. Conclusions

In this paper, a novel damage detection method was proposed based on the damage-induced chord-wise deflections which were estimated using the modal flexibility matrices before and after damage.

A new load concept, so called Positive Bending Inspection Load (PBIL) was proposed to make the proposed damage detection and localization procedures effective. A PBIL in an inspection region is defined as a load or a system of loads which guarantees positive bending moment in the inspection region of a structure. The relationship between the damage location and the damage-induced chord-wise deflection (DI-CD) was theoretically investigated, and it was proved analytically that the DI-CD has the maximum value at the true damage location with the abrupt change in its slope under a PBIL.

Novelty indices defined based on the damage-induced chord-wise deflection were devised for assessing damage existence under inevitable measurement noises and the index of the abrupt change in the slope of DI-CD were also proposed for damage localization. From a numerical study, the effectiveness of the proposed method of detecting small local damages has been demonstrated on a simply supported beam and a three span continuous beam. Then, experimental verifications were carried out for a two-span continuous steel-box girder model. It has been founded that the proposed method can detect small narrow cuts inflicted on the bottom flange which caused 12% reduction in the bending rigidity ( $EI$ ) on the narrow segment of the box-girder.

## Acknowledgement

This research is supported by the Smart Infra-Structure Technology Center (SISTeC) at KAIST established by Korea Science and Engineering Foundation (KOSEF) under grants R11-2002-101-00000-0, and also supported by the Korea Research Institute of Standard and Science (KRISS) under grants NEMA-05-MD-02. Their financial supports are greatly acknowledged.

## References

- Bernal, D. (2002), "Load vectors for damage localization", *J. Eng. Mech. ASCE*, **128**(1), 7-14.
- Bernal, D. (2004), "Modal scaling from known mass perturbations", *J. Eng. Mech. ASCE*, **130**(9), 1083-1088.
- Brincker, R., Zhang, L. M. and Andersen, P. (2001), "Modal identification of output-only systems using frequency domain decomposition", *Smart Mater. Struct.*, **10**(3), 441-445.
- Brinker, R. and Andersen, P. (2002), "A way of getting scaled mode shapes in output-only modal testing", 21th Modal Analysis Conf. (IMAC XXI), Paper No. 141 (CD-Rom), Orlando, FL.
- Doebeling, S. W., Farrar, C. R., Prime, M. B. and Shevitz, D. W. (1996), *Damage Identification and Health Monitoring of Structural and Mechanical Systems from changes in their Vibration Characteristics: A Literature Review*. Los Alamos National Laboratory Report LA-13070-MS.
- Duan, Z. D., Yan, G. R., Ou, J. P. and Spencer, B. F. (2005), "Damage localization in ambient vibration by constructing proportional flexibility matrix", *J. Sound. Vib.*, **284**(1-2), 455-466.
- Gao, Y., Spencer, B. F. and Ruiz-Sandoval, M. (2006), "Distributed computing strategy for structural health

- monitoring”, *Struct. Cont. Health Monit.*, **13**(1), 488-507.
- Kim, B. H., Joo, H. J. and Park, T. (2007), “Damage evaluation of an axially loaded beam using modal flexibility”, *J. Korean Society of Civil Eng.*, **11**(2), 101-110.
- Lee, J. J. and Yun, C. B. (2007), “Damage localization for bridges using probabilistic neural networks”, *J. Korean Society of Civil Eng.*, **11**(2), 111-120.
- Madhwesh, R. and Ahmet, E. A. (1992), “Flexibility by multireference impact testing for bridge diagnostics”, *J. Struct. Eng.*, **118**(8), 2186-2203.
- Ni, Y. Q., Zhou, H. F., Chan, K. C. and Ko, J. M. (2008), “Modal flexibility analysis of cable-stayed bridge for damage identification”, *Comput. Aid. Civ. Infrastr. Eng.*, **23**(3), 223-236.
- Pandey, A. K. and Biswas, M. (1994), “Damage detection in structures using changes in flexibility”, *J. Sound. Vib.*, **169**(1), 3-17.
- Peeters, B. and De Roeck, G. (2001), “Stochastic system identification for operational modal analysis: A review”, *J. Dynamic Sys. Measurement Control-Transactions, ASME*, **123**(4), 659-667.
- Toksoy, T. and Aktan, A. E. (1994), “Bridge-condition assessment by modal flexibility”, *Experimental Mech.*, **34**(3), 271-278.
- Yan, A. M. and Golinval, J. C. (2005), “Structural damage localization by combining flexibility and stiffness methods”, *Eng. Struct.*, **27**(12), 1752-1761.
- Yi, J. H. and Yun, C. B. (2004), “Comparative study on modal identification methods using output-only information”, *Struct. Eng. Mech.*, **17**(3-4), 445-466.
- Zhang, Z. and Aktan, A. E. (1995), “The Damage Indices for the constructed facilities”, *The 13th International Modal Analysis Conference (IMAC)*, 1520-1529.
- Zhao, J. and DeWolf, J. T. (1999), “Sensitivity study for vibrational parameters used in damage detection”, *J. Struct. Eng. ASCE*, **125**(4), 410-416.

## Appendix Proof for Eq. (18)

### A.1. Proof for span inspection region

Consider an equivalent simple beam with end rotational springs subjected to damage as shown in Fig. 2(a). Herein, the span inspection region is  $\Omega=[0, L]$ . Then, the chord-wise deflection  $\Delta u_{\Omega}(x)$  is identical to the deflection  $\Delta u(x)$ . Thus, the proof will be carried out on  $\Delta u(x)$  instead of  $\Delta u_{\Omega}(x)$ .

#### A.1.1. Sufficiency ( $\Rightarrow$ )

The first statement “ $\Delta u_{\Omega}(x)$  has maximum at  $x = x_D$  under a PBIL” can be proved by showing the following inequality to hold,

$$\Delta u(x_D) - \Delta u(x) \geq 0 \quad \text{on} \quad x \in [0, L] \quad (26)$$

For the domain  $0 \leq x < x_D$ , Eq. (26) can be rewritten using Eqs. (10), (14), and (16) as

$$\Delta u(x_D) - \Delta u(x) = \frac{\theta_{A1}}{3EI} \frac{(x_D - x)}{(4 + 4k_A + 4k_B + 3k_A k_B)x_E L^2} \times P_1(x) \quad (27)$$

where

$$P_1(x) = a_1 x^2 + b_1 x + c_1$$

$$a_1 = -2x_E k_A + 2x_D k_B + 3(x_D - x_E)k_A k_B$$

$$b_1 = 2x_E k_A (2x_D + 3k_E)k_A + 2x_D^2 k_B + 6x_E^2 k_A k_B > 0$$

$$c_1 = 4x_E L^2 + 2x_D (2L + x_E)k_A + 2x_E^2 (2L + x_D)k_B + 6x_D k_E k_A k_B > 0, \text{ and}$$

$\theta_{A1} > 0$  under a PBIL as discussed in Section 2.4.

All the terms in Eq. (27) are obviously positive except  $P_1(x)$ . Thus, the positiveness of  $P_1(x)$  is needed to be shown. It can be easily shown that  $P_1(x)$  is positive at two boundary points at  $x = 0$  and  $x_D$  as.

$$P_1(0) = c_1 > 0$$

$$P_1(x_D) = 4x_E L^2 + k_A \cdot 6x_D x_E (x_D + 2x_E) + k_B (4x_D^3 + 6x_D x_E^2 + 4x_E^3) + k_A k_B \cdot 3x_D (x_D^2 - x_D x_E + 4x_E^2) > 0$$

For the case of  $a_1 > 0$ , the global minimum of  $P_1(x)$  occurs at  $x_m = -b_1/(2a_1)$ , which is outside of the region of  $0 \leq x \leq x_D$ . Thus,  $P_1(x) > 0$  in the region since it is second order polynomial. For the case of  $a_1 < 0$ ,  $P_1(x)$  is a convex or linear curve so  $P_1(x) > 0$  for  $0 \leq x \leq x_D$ . Therefore,  $P_1(x) > 0$  and the r.h.s. of Eq. (27) is positive.

For the other domain of  $x_D \leq x \leq L$ , a similar procedure can be shown for Eq. (26). Thus,  $\Delta u(x)$  has been proven to have the maximum at  $x = x_D$ .

The second statement that “ $\Delta u'(x)$  changes abruptly at  $x = x_D$  under a PBIL” is obvious, since there is the abrupt change in  $\Delta u'_1(x)$  as shown in Fig. 3.

#### A.1.2. Necessity ( $\Leftarrow$ )

Contraposition of the necessity is written as.

$$\text{Damage doesn't occurs at } x = x_D \Rightarrow \begin{cases} \Delta u_D(x) \text{ doesn't has the maximum at } x = x_D \text{ or} \\ \Delta u'_D(x) \text{ doesn't changes abruptly at } x = x_D \text{ under a PBIL} \end{cases}$$

The proof for the necessity can be done by showing the above statement and is very obvious.

#### A.2. Proof for intermediate support inspection region

Consider a continuous beam system with damage loaded by a PBIL as shown in Fig. A-1. Herein, the intermediate support inspection region is  $\Omega = [x_a, x_b]$ , where  $x_a = 3/4 L_1$ , and  $x_b = L_1 + 1/4 L_2$ . Without loss of generality, the damage is assumed to locate in the left span region near the intermediate support,  $x_D \in [x_a, L_1]$ .

The continuous beam can be regarded as two equivalent single-span beams with rotational springs as show in Fig. A-2. Then, the damage induced deflection in the left span can be derived from Eqs. (10), (14) and (16). On the other hand, the damage-induced deflection in the right span can be obtained by using the rotational compatibility condition at  $x = L_1$ ; i.e.,  $\Delta u'(L_1^+) = \theta_B$  as

$$\Delta u(x) = \theta_B (x - L_1) (L_1 + L_2 - x) \left( \frac{1}{L_2} - \frac{1 + k_n}{2 + k_n} (x - L_1) \right) \quad (28)$$

where  $k_n = \frac{k_C}{2E_2 I_2 / L_2}$ ,  $E_2$  and  $I_2$  is the Young's modulus and moment of inertia in the right span, respectively;

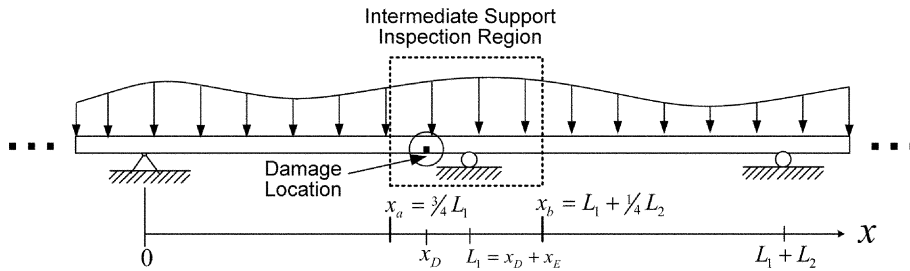


Fig. A-1 Damage-induced deflection near an intermediate support

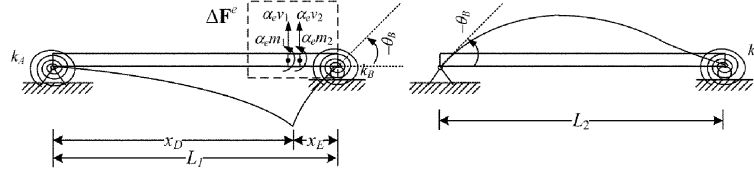


Fig. A-2 Equivalent single-span beams for the left and right spans

$\theta_B < 0$  under a PBIL as discussed in Section 2.4.

#### A.2.1. Sufficiency ( $\Rightarrow$ )

The curvature  $\kappa(x)$  in the left span can be obtained by differentiating Eq. (16) twice, as

$$\kappa(x) = 6\theta_{A1} \frac{k_A 2L_1 x_E + k_B(-x_D^2 + x_D x_E + 2x_E^2) + (x - x_D - x_E)(-2k_A x_E + 2k_B x_D + k_A k_B 3(x_D - x_E))}{x_E L^2 (4 + 4k_A + 4k_B + 3k_A k_B)}$$

where  $\kappa(x)$  can be shown to be positive for  $x \in [x_a, L_1]$  since  $\kappa(x)$  is the 1<sup>st</sup> order polynomial with positive values at two boundary points at  $x = x_a$  and  $L_1$  as.

$$\kappa(x_a) = C \left[ k_A \frac{1}{2} x_E L_1 + k_B \frac{3}{2} x_D L_1 + k_A k_B \frac{1}{4} (5x_D - x_E) L_1 \right] > 0, \text{ and}$$

$$\kappa(L_1) = C [k_B 2x_D L_1 + k_A k_B (2x_D - x_E) L_1] > 0$$

in which  $C = 6\theta_{A1} / [x_E L^2 (4 + 4k_A + 4k_B + 3k_A k_B)]$

By differentiating Eq. (28) twice, the  $\kappa(x)$  for  $x \in [L_1, x_b]$  can be obtained as

$$\kappa(x) = \theta_B \frac{-2(3 + 2k_n)L_2 + 6(1 + k_n)(x - L_1)}{(2 + k_n)L_2^2}$$

where  $\kappa(x)$  can be shown to be positive for  $x \in [L_1, x_b]$  since  $\theta_B < 0$  under a PBIL and  $\kappa(x)$  is the 1<sup>st</sup> order polynomial of  $x$  with positive values at two boundary points  $x = L_1$  and  $x_b$  as

$$\kappa(L_1) = -\theta_B \frac{6 + 4k_n}{L_2(2 + k_n)} > 0 \quad \text{and} \quad \kappa(x_b) = -\theta_B \frac{9 + 5k_n}{L_2(4 + 2k_n)} > 0$$

Therefore,  $\kappa(x)$  is positive for the whole intermediate support inspection region except the damage location  $x = x_D$

$$\kappa(x) > 0, \quad x \in [(x_a, x_D) \cup (x_D, x_b)] \quad (29)$$

Furthermore, the following two inequalities hold according to the previous proof in Appendix A-1 and the fact that  $\Delta u(x_b)$  is negative since  $\theta_B < 0$  as

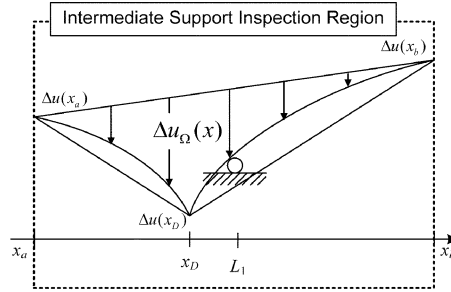


Fig. A-3 Chord-wise deflection in an intermediate support region

$$\Delta u(x_D) > \Delta u(x_a) \quad \text{and} \quad \Delta u(x_D) > 0 > \Delta u(x_b) \quad (30)$$

From Eqs. (29) and (30), the deflection curve can be depicted as follows.

Accordingly, it can be found that the maximum chord-wise deflection  $\Delta u_\Omega(x)$  occurs at  $x = x_D$  regardless of the magnitude of  $\kappa(x) > 0$ .

The proof of the abrupt change in  $\Delta u'_\Omega(x)$  for the intermediate support region is obvious since there is an abrupt change in  $\Delta u'_1(x)$  as shown in Fig. 3.

#### A.2.2. Necessity ( $\Leftarrow$ )

The proof for the intermediate support region can be done by proving the contraposition of the necessity and is very obvious.